Modelling of SO_3 Formation in the Flame of a Heavy-oil Fired Furnace

D. R. Schneider* and Ž. Bogdan
Power Engineering Department, Faculty of Mechanical Engineering and Naval Architecture, University of Zagreb,
I. Lučića 5, 10000 Zagreb, Croatia
E-mail: daniel.schneider@fsb.hr

Original scientific paper
Received: October 15, 2002
Accepted: May 22, 2003

The accurate description of sulphur trioxide formation in the flame is a prerequisite for developing a realistic SO_3 model that could be used in an analysis of reduction of low-temperature corrosion in steam generators. The scope of this paper is limited only to SO_3 produced in the furnace by homogenous gas-phase reactions during heavy-oil fuel combustion and does not include heterogeneous catalytic reactions on heat exchanger's surfaces and ash particles. As a first attempt, SO_3 was modelled as a part of globally applied combustion model – the probability density function/equilibrium chemistry model. By comparison with known data, it was concluded that this model does not give realistic results. An extensive literature review revealed dominant reactions in which SO_3 participates. Further analysis showed that the SO_3 reactions could be considered as slow ones comparing to the main reactions during combustion, which means that the chemical equilibrium assumption could not be employed. Based on these reactions, a new SO_3 model, which takes into account finite kinetic character of reactions, was defined. It was implemented into the Fluent™ CFD code as a user subroutine. Such mathematical model was used for simulation of a full-scale furnace of the oil-fired steam generator. The accuracy of the model was assessed by comparison with measured data and available data from the literature. Satisfying conformance was established.

Keywords:
SO_3, numerical modelling, furnace, heavy-oil fuel combustion

Introduction

The necessity for the accurate prediction of SO_3 formation arose in a study of reduction of low-temperature corrosion in the oil-fired power plant steam generator.[1] During combustion of heavy-oil fuel, rich in sulphur, certain amount of produced SO_2 (typically 1–3 %) is being transformed into SO_3, which at lower temperatures (below approx. 580 °C), reacts with water vapour forming sulphuric acid[2]

$$SO_3 + H_2O \rightleftarrows H_2SO_4 \qquad (1)$$

If the temperature of flue gases, containing H_2SO_4 and H_2O vapours, lowers below the dew point, it results in condensation on the heat exchanger surfaces. Combination of H_2SO_4 and H_2O

$$H_2SO_4 + 2H_2O \rightleftarrows 2H_3O^+ + SO_4^{--} \qquad (2)$$

with the surface metal creates an electrolytic system in which metals turn into their salts, i.e. the low-temperature corrosion, which impairs the steam generator components, occurs.

The sulphur trioxide primarily forms within the flame by homogenous gas-phase reactions involving oxygen radical. A proof for this statement could be found in the fact that there is no any SO_3 formed in stoichiometric combustion ($\lambda = 1.0$). Unfortunately, such combustion is not viable in commercial steam-generators due to the rise in CO and soot and therefore certain air surplus must exist. On the other hand, the heavy oil fuel of lower quality, which is typically used in power plants due to economical reasons, contains, besides sulphur, metals like vanadium (V) and iron (Fe). Those elements could react with the oxygen from combustion air surplus creating oxides of V_2O_5 and Fe_2O_3 that form layers on the heat exchanger's surfaces. The vanadium pentoxide (V_2O_5) acts as a catalyst in the temperature range of 500 and 800 °C accelerating the SO_3 formation. Thus formed SO_3 can exceed the SO_3 produced in the flame by factor two or three[3]. Since this study was limited to analysis of SO_3 formation in the furnace, it was assumed that the steam-generator in consideration was in its clean condition i.e. at the moment when the oxide scales on heat exchanger's surfaces are not yet formed.

Modelling of SO_3 formation has been investigated in context of a study of detailed 3D mathematical model of the furnace, which had been set using the Fluent™ CFD code.[4] In version (v6.0) several different combustion models are at disposal,

* Corresponding author

which could be used for description of sulphur trioxide generation. Generalized finite-rate models (Arrhenius finite-rate, Magnussen eddy dissipation and EDC model)[5] do not accurately represent turbulent diffusion flames and also engage solving of up to the hundred chemical species' transport equations. That, apart from requirement for great processing power, also induces high non-linearity of solution and deteriorates convergence. Unlike those models, the probability density function model (PDF)[6] is specifically developed for the simulation of turbulent diffusion flames and offers many benefits over the finite-rate formulation. The PDF model has also been chosen in the present study as the global combustion model. The effects of the turbulent fluctuations of main combustion variables (species concentrations, density and temperature) are accounted for with statistical approach of PDF. Reaction mechanism is not explicitly defined; instead, the reacting system is described by the equilibrium chemistry formulation,[7] which implicates that the chemistry is fast enough to preserve chemical equilibrium at the molecular level. This assumption is valid for the main reactions and species in the combustion process but it fails in the case of slow kinetics like the one of NO_x and SO_3 formation. Better choice of combustion model would be the laminar flamelet model,[8] which as extension of the PDF model could account for aerodynamic strain-induced departure from chemical equilibrium. The problem is that the present version of laminar flamelet does not include the unsteady concept, which could only be used for prediction of slowly reacting chemical species such as NO, CO, soot and SO_3 where unsteady effects are important.

These were reasons that urged a development of separate SO_3 formation model that was finally implemented into the global Fluent™ CFD code.

Mathematical Model

Reaction mechanism

As it was said in the introduction, the present study focuses on sulphur trioxide produced within the flame by homogenous gas-phase reactions and does not include heterogeneous catalytic reactions on the heat exchanger's surfaces and ash particles. From a number of different reactions found in literature, two most important ones have been recognized[9]

$$SO_2 + O + M \underset{k_{3b}}{\overset{k_{3f}}{\rightleftharpoons}} SO_3 + M \qquad (3)$$

$$SO_3 + O \underset{k_{4b}}{\overset{k_{4f}}{\rightleftharpoons}} SO_2 + O_2 \qquad (4)$$

where the recommended values[10] for third body reactants M are: N_2 /1.3/, SO_2 /10.0/, H_2O /10.0/.

Proposed SO_3 model is based on the assumption that the sulphur trioxide could be examined independently of the complete reaction set, whereby all other molecular species (calculated with the PDF/equilibrium chemistry combustion model) are maintained at constant concentrations. That is correct for low conversion of SO_2 to SO_3 (lower than 5 %)[9] as it is the case for typical combustion processes in furnace. The rate of change of SO_3 concentration for reactions (3) and (4) is

$$\frac{\mathrm{d}c_{SO_3}}{\mathrm{d}t} = k_{3f} c_{SO_2} c_O c_M + k_{4b} c_{SO_2} c_{O_2} - k_{3b} c_{SO_2} c_M - k_{4f} c_{SO_2} c_O \qquad (5)$$

where k_{3f}, k_{4f} are the rate coefficients for forward reactions given by[11,12]

$$k_{3f} = 9.2 \cdot 10^{10} \exp\left(\frac{-1200.38}{RT}\right) \qquad (6)$$

$$k_{4f} = 2 \cdot 10^{12} \exp\left(\frac{-10064.95}{RT}\right) \qquad (7)$$

The rates for reverse reactions (3) and (4) are obtained from the equilibrium constants $K_{c,i}$ for each chemical reaction i

$$k_{ib} = \frac{k_{if}}{K_{c,i}}, \qquad i = 3,4 \qquad (8)$$

which could be calculated from the molar Gibbs energy of considered reaction

$$K_{c,i} = (RT)^{-\sum_{k=1}^{S}(\nu_{k,i}^n - \nu_{k,i}^r)} \exp\left\{-\left[a_{1,i}^r(1-\ln T) - \frac{a_{2,i}^r}{2}T - \right.\right.$$
$$\left.\left. - \frac{a_{3,i}^r}{6}T^2 - \frac{a_{4,i}^r}{12}T^3 - \frac{a_{5,i}^r}{20}T^4 + \frac{a_{6,i}^r}{T} - a_{7,i}^r\right\}\right] \qquad (9)$$

The polynomial coefficients for reactions (3) and (4) $a_{l,i}^r$ (l = 1,..,7) are given in Table 1. They were obtained from the polynomial coefficients[13] for standard molar specific enthalpies and entropies of the species formation $a_{l,k}$ together with the stoichiometric coefficients ν_{ki}

$$a_{l,j}^r = \sum_{k=1}^{S} (\nu_{ki}^n - \nu_{ki}^r)\, a_{l,k} \qquad (10)$$

Special attention was given to calculation of O radical, which is (besides temperature) one of the most important factors that determine SO_3 production in the flame. Since, at present, there is no final conclusion on which approach to O modelling in

Table 1 – *Polynomial coefficients for reactions (3) and (4)*

Reaction	a_1^r	a_2^r	a_3^r	a_4^r	a_5^r	a_6^r	a_7^r
(3)	-6.41E-01	-6.27E-04	4.66E-07	-1.01E-10	7.52E-15	-1.78E+04	8.19E+00
	6.03E-01	-4.28E-03	2.40E-06	2.01E-09	-1.62E-12	-1.81E+04	1.99E+00
(4)	-7.46E-01	1.30E-03	-5.85E-07	1.10E-10	-7.78E-15	-4.19E+04	-1.48E+01
	-3.28E+00	8.69E-03	-7.81E-06	2.51E-09	-3.80E-14	-4.12E+04	-1.89E+00

turbulent diffusion flames is the most appropriate, three different methods were investigated. According to *Westenberg*[13], the O atom concentration can be calculated from the expression based on assumption of O in equilibrium with O_2

$$c_O = 3.97 \cdot 10^5 T^{-0.5} c_{O_2}^{0.5} \exp\left(\frac{-31090}{T}\right) \quad (11)$$

that corresponds to the reaction

$$O_2 \Leftrightarrow O + O \quad (12)$$

This approach will be referred later in the text as the *full equilibrium O approach*. A modification of the previous method can be made by introducing third-bodies in the reaction (12)

$$O_2 + M \Leftrightarrow O + O + M \quad (13)$$

The concentration of O in such dissociation-recombination process can be obtained from the expression

$$c_O = 36.64 T^{0.5} c_{O_2}^{0.5} \exp\left(\frac{-27123}{T}\right) \quad (14)$$

This approach is named after lying assumption of partial equilibrium of O with O_2 as the *partial equilibrium O approach*. The third approach is based on the hypothesis of the total equilibrium of all species in the mixture. Since combustion model employed (PDF/equilibrium chemistry model) uses the very same definition, the O concentration could be simply taken from converged solution of the global reactive system as

$$c_O = \overline{w}_O \frac{\rho}{M_O} \quad (15)$$

where the mean O mass concentration is now only a function of the mean mixture fraction, its variance and the enthalpy

$$\overline{w}_{O,t} = \overline{w}_O(\bar{f}, \overline{f'^2}, \overline{H}^*) \quad (16)$$

This method will be considered as the *predicted O approach*. In the case of all three approaches all other species concentrations that appear in expression (5) (SO_2, O_2 and species representing third-bodies) are also taken from converged solution of the combustion model.

Transport equation

The steady-state transport equation for SO_3 is written in the following form

$$\rho u_i \frac{\partial w_{SO_3}}{\partial x_i} = \frac{\partial}{\partial x_i}\left(\frac{\mu_{eff}}{\sigma} \frac{\partial w_{SO_3}}{\partial x_i}\right) + \Gamma_{SO_3} \quad (17)$$

where Schmidt-Prandtl number σ = 0.7. The left hand side term of the equation (17) represents transport of SO_3 by convection, while the first term on the RHS is diffusion of SO_3. The second term Γ_{SO_3} in the equation is source of SO_3 by chemical reaction and it is defined as

$$\Gamma_{SO_3} = \frac{\partial}{\partial t}(\rho w_{SO_3}) \quad (18)$$

Relation between the SO_3 mass fraction w_{SO_3} and the concentration c_{SO_3} is given by

$$w_{SO_3} = \frac{M_{SO_3}}{\rho} c_{SO_3} \quad (19)$$

Finally, one gets

$$\Gamma_{SO_3} = M_{SO_3} \frac{dc_{SO_3}}{dt} = M_{SO_3}(k_{3f} c_{SO_2} c_O c_M + k_{4b} c_{SO_2} c_{O_2} - k_{3b} c_{SO_3} c_M - k_{4f} c_{SO_3} c_O) \quad (20)$$

Model implementation

The SO_3 model is implemented into the Fluent CFD code as the User Defined Function routine. The global 3D mathematical model of the furnace comprises coupled gas flow and liquid spray physics in the non-premixed turbulent flame. Transport of mass, momentum, energy and chemical species (only NO, soot and SO_3) in the gas phase is ob-

tained by solving standard Favre-averaged Eulerian conservation equations[5]. Turbulent flow is modelled by the realizable *k-ε* model. The pressure field is calculated from the continuity equation using the PISO algorithm. The heavy fuel oil spray is described as a discrete second phase using "particle-in-cell model"[15] dispersed in continuous (gas) phase. Trajectories, mass, momentum and heat balance equations for the particles, i.e. fuel droplets, are solved in the Lagrangian frame of reference. The turbulent dispersion of droplets is predicted using the stochastic "random walk" (or "eddy lifetime") model. The radiation heat transfer is described with the discrete ordinates radiation model, which could account for particulate effects between gas and droplets. The absorption coefficient of the mixture is calculated as the weighted-sum-of-grey--gases. The soot formation is modelled on the basis of the simple single-step model of *Khan* and *Greeves*[16]. The formation of NO_x is attributed to three reaction mechanisms: thermal (also known as extended Zeldovich mechanism[17]), prompt and fuel NO_x mechanism.

Taking the assumption of SO_3 concentration independency, the SO_3 UDF subroutine could be solved in post-processing stage, after converged solution of global CFD model is obtained. The linearized transport equation for SO_3 has a following form

$$a_P (w_{SO_3})_P = \sum a_{NP} (w_{SO_3})_{NP} + \Gamma_{SO_3} \quad (21)$$

A special attention has to be paid to linearization of the source term

$$\Gamma_{SO_3} = (\Gamma_{SO_3})_{old} + \frac{\partial \Gamma_{SO_3}}{\partial w_{SO_3}} [(w_{SO_3})_P - (w_{SO_3})_{P,old}] \quad (22)$$

where the implicit part of the source term should be prescribed as

$$\frac{d\Gamma_{SO_3}}{dw_{SO_3}} = \frac{d}{dw_{SO_3}} \left[\frac{d(\rho w_{SO_3})}{dt} \right] = \frac{\rho^2}{M_M} k_{3b} w_M - \rho k_{4f} w_O \quad (23)$$

The final form of linearized equation could be written as

$$\left(a_P - \frac{\partial \Gamma_{SO_3}}{\partial w_{SO_3}} \right) (w_{SO_3})_P = \sum a_{NB} (w_{SO_3})_{NB} + \left[(\Gamma_{SO_3})_{old} - \frac{\partial \Gamma_{SO_3}}{\partial w_{SO_3}} (w_{SO_3})_{P,old} \right] \quad (24)$$

where the subscripts *P* and *NP* indicate values of variable at the central and neighbouring nodes while subscript *old* signs value from the previous iteration.

Results and discussion

Described mathematical model has been applied to simulate the SO_3 formation in the furnace of the steam-generator of PP Sisak. The furnace has dimensions of 8.4 × 8.4 × 25.1 m and enables thermal input of 300 MW_t. On each side-wall of the chamber, at height of approx. 2 m, there are two oil burners. The burner consists of an axial/radial inflow type swirl generating register and a steam atomiser. The fuel is heavy-oil fuel of composition 84.69 % C, 11.53 % H, 0.78 % N, 0.78 % O and 2.23 % S. The oil preheated to 125 °C at 20 bar is atomised into fine mist by steam at 8.5 bar and 273 °C in so called Y-nozzles. Detailed description, with the furnace and burner geometry together with the boundary conditions, can be found in previous papers.[1,4]

The results of simulations are compared to the data measured in operational conditions. The steam-generator operated at 73.3 % load. The air excess ratio had been increased from value that corresponds to 0.8 % O_2 measured in the flue gases up to 3.2 % O_2. SO_3 at the exit was measured with the Gallenkamp™ GC-220 sulphur oxide analyser according to EPA 8 method. The O_2 content, like the other main combustion parameters, was assessed by the standard flue gas analyser RBR-ECOM™-SG^{PLUS}. Following picture (Fig. 1) shows the comparison of measured data with results of three different variants of SO_3 model that differ in approach to calculation of oxygen atom concentration. As it can be seen from the diagram, there is considerable scattering of measured data (hollow diamond markers), which is not unusual taking into account the nature

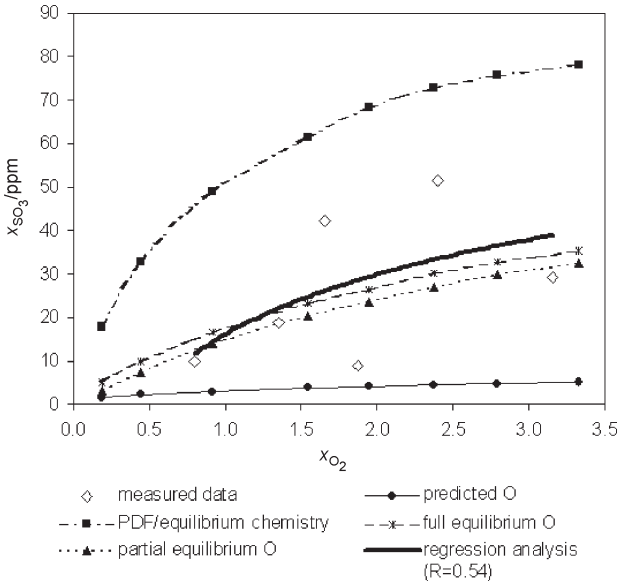

Fig. 1 – *Predicted and measured SO_3 vs. O_2 mole fractions*

of measuring method[18]. The regression analysis (R = 0.54) revealed expected[2,18,19] trend of increase of SO_3 with the increase of air excess ratio, manifested in higher O_2 content. At that time it was not possible to determine what was the contribution of catalytic SO_3 in total measured SO_3 if it was such one. Therefore the absolute values of SO_3 must be taken with scrutiny while the trend of SO_3 increase can be accepted as valid. The SO_3 mole fractions obtained by the PDF/equilibrium chemistry combustion model (full square symbols) show significant deviation from the measured data. The mathematical model of SO_3 formation, in which the O concentration is taken from converged solution (predicted O approach), gives the mole fractions of sulphur trioxide that are much lower than the data measured on the steam-generator (solid line with full circle markers, Fig. 1). The values of SO_3, calculated by the models with full and partial equilibrium O approach (full triangle and asterisk symbols, respectively), are in far better accordance to the measured SO_3 mole fractions. Since the SO_3 model based on the assumption of full equilibrium of O offers slightly higher compliance, it was chosen as the model preferred in this study. Applying that model as the part of a global mathematical model of the furnace, the SO_3 profile along the furnace was calculated. Figure 2 shows the percentage of conversion of SO_2 to SO_3 plotted against the flue gas path through the furnace and horizontal connective channel. The graph refers to the case that corresponds to 3.3 % O_2 by volume at the exit.

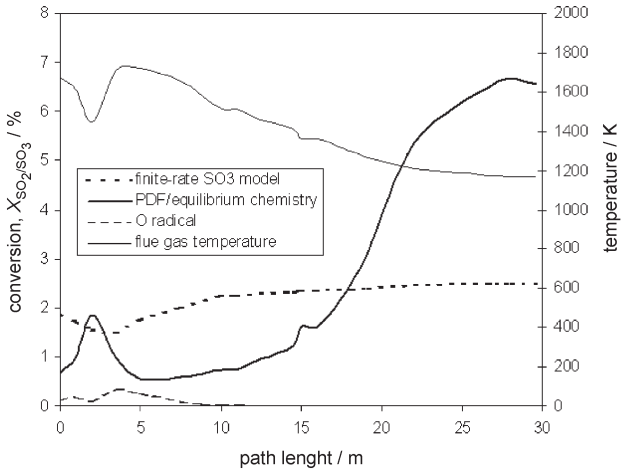

Fig. 2 – *SO_3 conversion vs. flue gas path through the furnace and connective channel*

The solid line represents the SO_3 conversion obtained by the PDF/equilibrium chemistry model while dotted line comprises the values calculated by the SO_3 model with the assumption of O in full equilibrium with O_2. The temperature and radical O profile are represented by thin solid and broken line, respectively. All variables are averaged on cross-sections of furnace along the path of flue gases. At high temperatures in the flame (1400 to 1800 K), i.e. between 3 and 17 m of furnace height, the SO_3 content (also SO_3 conversion) calculated by model that takes into account the SO_3 reaction kinetics is higher than values obtained by PDF/equilibrium chemistry model. That could be explained by the fact that the actual O atom concentration in the flame is higher than the equilibrium one. At the same time, the equilibrium chemistry assumption implicates that all other species in the mixture are in equilibrium and all reactions are equilibrated. If one of the species, in particular CO, has a slower rate of reaction, the remaining much faster reactions assume different pseudo-equilibrium. When the main combustion reactions finish, the oxygen atom concentration returns to equilibrium with O_2 , and SO_3 produced in the flame can be reconverted to SO_2.

At lower temperatures (1200 to 1300 K), i.e. above 17 m of furnace height, the amount of equilibrium SO_3 suddenly raises to almost 7 % of SO_3 conversion at the furnace exit. This is unrealistically high value, what it could be confirmed by data measured at the exit (Fig. 1) and also from the literature. Hedley has showed in his paper[19] the measured (dotted line) and theoretical equilibrium (solid lines) SO_3 conversion data for a typical steam-generator (Fig. 3). A partial qualitative conformance could be observed. Quantitative differences were expected because Hedley's profiles extend over entire steam-generator (and different temperature range, consecutively), while the scope of this paper is the furnace. A significant discordance occurs at approx. 2 m of furnace height. A high peak on the equilibrium chemistry curve (thick solid line, Fig. 2) and the slight drop in the finite-rate SO_3 model curve (dotted line, Fig. 2), compared to the SO_3 conversion curves on Fig. 3, are due to lower temperatures (thin solid line,

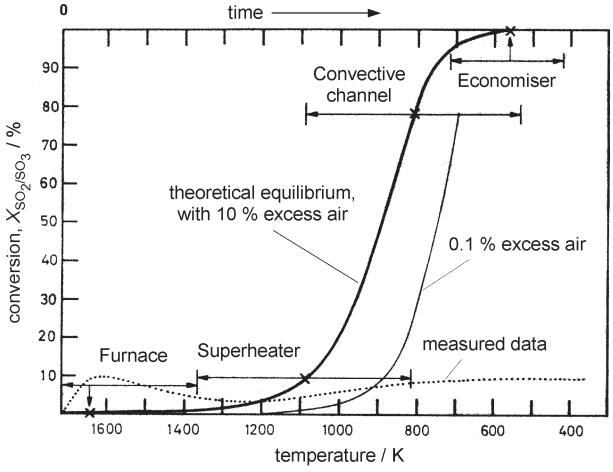

Fig. 3 – *Measured and theoretical equilibrium SO_3 conversion for a typical steam-generator*

Fig. 2) in front of the burners that supply furnace with relatively cold air (T = 528 K). The difference follows from the fact that the chosen variable for the abscissa in the Hedley's diagram is the temperature, while in graph on Fig. 2 it is the flue gas path length. Better agreement can be achieved comparing Hedley's measured data to the results of finite-rate SO_3 model plotted against the temperature (Fig. 4). The dotted line (with triangle markers) represents the SO_3 formation rate (Eq. 25) calculated as the difference of production P_p and destruction P_d of sulphur trioxide

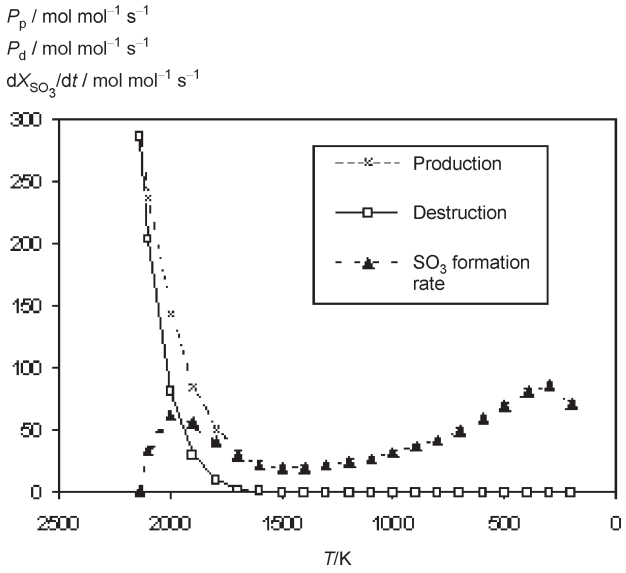

Fig. 4 – *Temperature dependency of SO_3 formation rate*

$$\frac{dx_{SO_3}}{dt} = P_p - P_d \qquad (25)$$

where P_p and P_d follow from equation (5) whereby concentrations are expressed as mole fractions

$$P_p = \frac{p}{RT}\left(k_{3f} x_{SO_2} x_O x_M \frac{p}{RT} + k_{4b} x_{SO_2} x_{O_2}\right) \qquad (26)$$

$$P_d = \frac{p}{RT}\left(k_{3b} x_{SO_3} x_M \frac{p}{RT} + k_{4f} x_{SO_3} x_O\right) \qquad (27)$$

The production, destruction and formation rate of SO_3 are shown (Fig. 4) as a function of temperature with constant values of x_O = 4.00E-9, x_{O2} = 3.81E-2, x_{SO2} = 1.10E-3 and x_M = 1, for initial SO_3 molar fraction in t = 0 of $x_{SO3} = x_{SO3,o}$ = 2.83E-5.

The O curve (dashed line, Fig. 2) possess local minimum at height that match burner plane what could be seen again to correspond to lower temperatures in the region. Since the calculation of O atom concentration is based on the full equilibrium approach, the equation (11) determines such temperature dependency. As the rate of change of SO_3 concentration (Eq. 5) is directly related to the O atom concentration, it can be stated that the SO_3 formation also depends on the amount of oxygen atoms.

The flow in the furnace is characterized by high turbulence (vorticity and recirculation) that determines complex 3D nature of SO_3 concentration pattern. Figure 5 shows the SO_3 mole fractions, calculated with the SO_3 finite-rate model, plotted in one vertical symetry plane dividing furnace, two lateral and one horizontal plane that section furnace along burners axes.

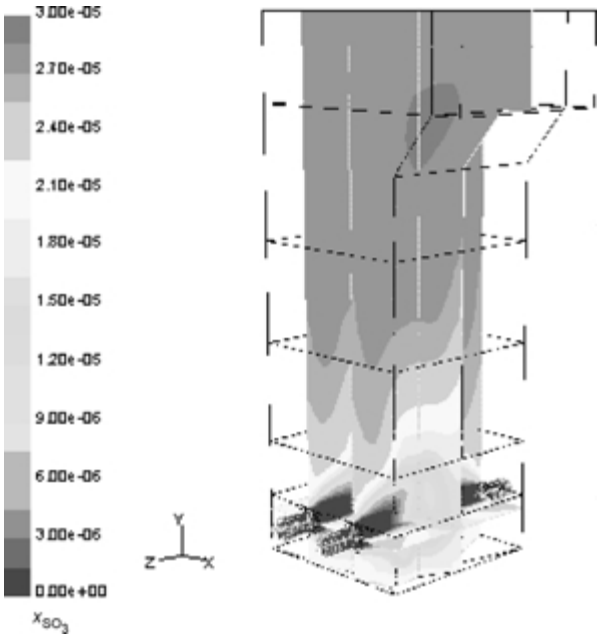

Fig. 5 – *SO_3 amount fractions in vertical plane dividing furnace, two lateral and one horizontal plane that section furnace along burners axes*

Conclusion

The in-flame SO_3 reaction mechanism was analysed. It was shown that the globally applied combustion model (PDF/equilibrium chemistry) could not be employed for description of the sulphur trioxide formation due to the finite kinetic character of SO_3 reactions. The finite-rate SO_3 model was defined and implemented into the Fluent™ CFD code as the UDF subroutine. The 3D mathematical model was used for simulation of the full-scale furnace of the oil-fired steam-generator. To avoid interference with the catalytically produced SO_3 a clean condition of the steam-generator was assumed.

Three different approaches to calculation of O radical were tested. The SO_3 model with full equilibrium O approach was chosen as the most representative one. Results obtained with that model rep-

licate the regression curve trend of measured SO_3 data with acceptable accuracy. The SO_3 conversion, temperature and O profiles along the furnace were presented. It was confirmed that the most important parameters influencing SO_3 formation are the temperature and availability of O atoms. Results of the model were qualitatively compared to the available data from the literature. Satisfying conformance was established. It could be concluded that proposed SO_3 model realistically simulate the SO_3 production in the flame. This model could be used as a base for the SO_3 model that would also include heterogeneous catalytic reaction mechanisms on the heat exchanger's surfaces and ash particles and that could be used in the analysis of reduction of the low-temperature corrosion in the steam-generators in real operating conditions.

Nomenclature

a – coefficient
– polynomial coefficient
c_i – concentration of species i, kg m^{-3}
$\bar{f}$ – mean of the mixture fraction
$\bar{f}'^2$ – variance of the mixture fraction
$\overline{H}^*$ – mean of enthalpy, J kmol^{-1}
k – reaction rate coefficient, (cm^3 mol^{-1})^n s^{-1}
– n = 1 for bimolecular reactions
– 2 for third body reactions
K_C – equilibrium constant, (mol m^{-3})$^{\Delta m}$
– Δm is sum difference of stoichiometric coefficients
M – molar mass, kg kmol^{-1}
p – pressure, Pa
P_d – destruction of SO_3, mol mol^{-1} s^{-1}
P_p – production and SO_3, mol mol^{-1} s^{-1}
R – universal gas constant, R = 1.987e-3 kcal mol^{-1} K^{-1} (8.314 J mol^{-1} K^{-1})
S – total number of chemical species
t – time, s
T – temperature, K
u – velocity, m s^{-1}
x – spatial coordinate, m
w_i – mass fraction of species i, kg kg^{-1}
x_i – mole fraction of species i, mol mol^{-1}

Greek Letters

σ – Schmidt-Prandtl number
Γ_i – source term of species i, kg m^{-3} s^{-1}
λ – air excess ratio
ρ – density, kg m^{-3}
μ – dynamic viscosity, Pa s
ν – stoichiometric coefficient

Subscripts

b – backward reaction
eff – effective
f – forward reaction
NP – neighbouring control volume
o – initial value
old – value from previous iteration
P – central control volume

References

1. *Schneider, D. R.,* Investigation of the Possibilities of SO_3 Reduction During Heavy Fuel Oil Combustion (in Croatian), PhD thesis, FSB, Zagreb, 2002
2. *Niepenberg, H. P.,* Industrie-Ölfeuerungen, Deutche Babcock & Wilcox, Oberhausen, 1968
3. *Adrian, F., und alle*, Jahrbuch der Dampferzeugungstechnik, 4. Ausgabe, Vulkan-Verlag, Essen, 1980
4. *Schneider, D. R., Bogdan, 4*., Transactions of FAMENA **26** (1) (2002) 15
5. FLUENT 6 User's Guide, Fluent Inc., Lebanon, NH, 1998
6. *Pope, S. B.,* Prog. Energy Combust. Sci. **11** (1986) 119
7. *Bilger, R. W.,* Turbulent flows with non-premixed reactants, in Libby, P. A. and Williams, F. A. (Ed.), Turbulent Reacting Flows, pp 65–114, Springer-Verlag, Berlin, 1980
8. *Peters, N.,* Prog. Energy Combust. Sci. **10** (1984) 319
9. *Hunter, S. C.,* Journal of Engineering for Power **104** (1982) 44
10. *Cullis, C. F., Mulcahy, M. F. R.,* Combustion and Flame, **18** (1972) 225
11. *Harris, B. W., Journal of Engineering for Gas Turbine and Power,* **112** (1990) 585
12. *De Blas, L. J. M.,* Pollutant formation and interaction in the combustion of heavy liquid fuels, PhD thesis, University College London, London, 1998
13. *Stull, D. R., Prophet, H.,* JANAF Thermochemical Tables, Office of Standard and Reference Data, NBS, Washington, D.C., 1971
14. *Westenberg, A. A.,* Comb. Sci. Tech., **4** (1971) 59
15. *Kuo, K. K.,* Principles of Combustion, John Wiley & sons, New York, 1986
16. *Khan, I. M., Greeves, G.,* A method for calculating the formation and combustion of soot in diesel engines, in Afgan, N. H. and Beer, J. M. (Ed.), Heat Transfer and Flames, Vol. 25, Scripta, Washington DC, 1974
17. *Bowman, C. T,* Progress in Engineering and Combustion Science, Pergamon Press Ltd., 1979
18. *Prelec, Z.,* Analiza stanja i način sanacije generatora pare u Termoelektrani Rijeka, studija, Savez energetičara Rijeka, Rijeka, 1992
19. *Hedley, A. B.,* Journal of the Institute of Fuel, **40** (1967) 142